

# Activity and Osmotic Coefficients of NaCl in Concentrated Solutions from 0 to $-40^{\circ}\text{C}$

Valerie L. Thurmond\* and Garrett W. Brass

Rosenstiel School of Marine and Atmospheric Science, University of Miami, Miami, Florida 33149-1098

A differential scanning calorimeter was used to measure specific heat capacity from cooling scans as a function of temperature and concentration. The heat capacity data were fit to the equations of Pitzer and co-workers to obtain activity and osmotic coefficients of NaCl and H<sub>2</sub>O, respectively, below 0 °C. Supercooling of the solutions was encouraged by using a fast scan rate (10° min<sup>-1</sup>) so that specific heat could be measured to lower temperatures than would be possible if the solutions were allowed to equilibrate with the solid phases. The solubility of ice was calculated and compared to the experimental freezing point in NaCl solutions.

## Introduction

Thermodynamic quantities of interest to solubility studies, e.g., activity coefficients, enthalpies, and heat capacities, change rapidly with concentration especially at low temperatures, yet there are very few measurements below 0 °C. We have measured heat capacities of sodium chloride solutions from 25 to  $-40^{\circ}\text{C}$  with a differential scanning calorimeter. Combining these results with literature values at 25 °C, we have calculated the activity coefficients from 0.5 *m* to saturation and down to  $-40^{\circ}\text{C}$  using Pitzer's equations (1-5).

## Experimental Section

The instrument used for measurement of specific heat was a standard Perkin-Elmer Model DSC-2. Although the DSC is not the most accurate instrument for certain types of calorimetric measurements, it is appropriate for the present purpose because heat capacities can be measured on solutions well below their normal freezing point by supercooling the solutions. The temperature that can be reached before freezing varies with the salt concentration. Typical thermograms are shown at several concentrations of NaCl in Figure 1. At 0.502 *m* the solution was cooled to about 250 K before freezing commenced, as shown by the large exotherm at 250 K. The thermogram for a 3.075 *m* solution shows that first ice, then a eutectic mixture of ice and solid sodium chloride, precipitates from the supersaturated solutions as the temperature decreases. With increasing concentration, the ice and eutectic exotherms are shifted to lower temperatures. In a 6.0 *m* solution, the solution remains supersaturated to below 230 K ( $-43^{\circ}\text{C}$ ) at which all of the runs were terminated.

The DSC-2 measures heat flow into or out of a sample per unit time ( $dH/dt$ ) relative to a known standard (usually sapphire). The specific heat ( $C_p$ ) is related to the heat flow by

$$\frac{dH}{dt} = mC_p \frac{dT}{dt} \quad (1)$$

The system collects data from the DSC and computes specific heat at 1-deg intervals. Energy calibration is afforded by data from a sapphire standard obtained over the same temperature range. Temperature is calibrated by measuring the melting temperatures of pure water and mercury at a scan rate of 5° min<sup>-1</sup> in the warming mode since freezing points measured from cooling scans are inaccurate due to supercooling. An empty aluminum sample pan is run to establish the baseline. The

Table I. Coefficients of Specific Heat Equations ( $C_p$  (cal g<sup>-1</sup> K<sup>-1</sup>) =  $a + bT + cT^2$ )

molality	<i>a</i>	<i>b</i>	<i>c</i>	$\sigma$
0.502	1.0188	$3.3706 \times 10^{-5}$	$-3.2140 \times 10^{-7}$	0.026
1.008	0.3541	$4.2178 \times 10^{-3}$	$-7.4560 \times 10^{-6}$	0.0035
1.995	-0.0208	$6.3853 \times 10^{-3}$	$-1.0972 \times 10^{-5}$	0.0085
2.558	-0.4040	$8.9889 \times 10^{-3}$	$-1.5687 \times 10^{-5}$	0.0037
3.075	-0.0829	$6.4988 \times 10^{-3}$	$-1.1247 \times 10^{-5}$	0.016
4.096	-0.3482	$8.2422 \times 10^{-3}$	$-1.4379 \times 10^{-5}$	0.0068
5.027	-0.3813	$8.5100 \times 10^{-3}$	$-1.5154 \times 10^{-5}$	0.011
6.002	-0.1433	$6.6580 \times 10^{-3}$	$-1.1863 \times 10^{-5}$	0.0085

samples, empty pan, and sapphire were all run at a scan rate of  $-10^{\circ}\text{min}^{-1}$  in the cooling mode at the highest instrument sensitivity (20 mcal s<sup>-1</sup>). Sample weights averaged 20 mg and were weighed on a Perkin-Elmer TGS-2 thermobalance precise to 0.1  $\mu\text{g}$ . A subambient kit was used which included a glovebox and helium purge gas supply.

Three samples were prepared at each concentration with different sample pans. The sapphire standard and empty pans were rerun before each set of three samples. Temperature was recalibrated from thermograms of mercury and pure water before and after the standards and samples were run. The temperature calibrations were reproducible to about 0.05 K.

## Results

The heat flow ( $dH/dt$ ) from each sample was converted to specific heat by eq 1. The specific heat values were smoothed over temperature by fitting the data to second degree polynomials. The coefficients of the smoothed specific heat equations and standard deviation for the three replicates at each concentration are given in Table I. Precision varies from about 0.4% to 2.6% of the average specific heat value with the most scatter at 0.502 *m*. Comparison of this data with literature values ( $\delta$ ) at 15 °C (Figure 2) shows that below 3.0 *m* the agreement is somewhat outside of the experimental uncertainty. Above 3.0 *m*, the accuracy cannot be determined since no literature data are available at high concentration. Although the errors are rather large, the DSC-2 permits measurement to temperatures below 0 °C and below the equilibrium freezing points.

The heat capacities measured in this study can be used to extend the ion interaction equations to temperatures below 0 °C. First, the specific heat of the sodium chloride solutions is converted to total heat capacity of an *m* molal solution containing 1 kg of water by

$$C_{p_i} = C_p(1000 + mM) \quad (2)$$

where *M* is the molecular weight of sodium chloride. The values of  $\bar{C}_{p_1}^0$  and  $\bar{C}_{p_2}^0$  are found by fitting  $C_{p_i}$  to eq 10 (Table II) and treating  $\bar{C}_{p_1}^0$ ,  $\bar{C}_{p_2}^0$ ,  $B_{mx}^j$ , and  $C_{mx}^j$  as adjustable parameters. A linear least-squares regression program (7) was used to fit the data. Below 0 °C the Debye-Hückel slope ( $A_\phi$  and  $A_j$ ) was extrapolated from the values of Silvester and Pitzer (5) above 0 °C.

The fitted values of  $\bar{C}_{p_1}^0$  and  $\bar{C}_{p_2}^0$  determined above were used to find the best values of the second temperature derivatives of  $\beta^{(0)}$ ,  $\beta^{(1)}$ , and  $C^\phi$  at each temperature. The heat capacity data was refit to eq 10 (Table II) by using the definitions of *J*,  $B_{mx}^j$ , and  $C_{mx}^j$  given in eq 11-13 (Table II). The values

**Table II. Pitzer's Equations for the Activity, Excess Free Energy, Enthalpy, and Heat Capacity of a Single Electrolyte<sup>a</sup>**

Osmotic Coefficient

(1)  $\phi - 1 = -|Z_m Z_x| A_\phi \frac{I^{1/2}}{1 + 1.2I^{1/2}} + \frac{m 2\nu_m \nu_x}{\nu} B_{mx}^\phi + m^2 \cdot 2 \frac{(\nu_m \nu_x)^{3/2}}{\nu} C_{mx}^\phi$

(2)  $B_{mx}^\phi = \beta^{(0)} + \beta^{(1)} \exp(-\alpha I^{1/2})$

Activity Coefficient

(3)  $\ln \gamma^\pm = -|Z_m Z_x| A_\phi \left[ \frac{I^{1/2}}{1 + 1.2I^{1/2}} + \frac{2}{b} \ln(1 + 1.2I^{1/2}) \right] + \frac{m \cdot 2\nu_m \nu_x}{\nu} B_{mx}^\gamma + m^2 \frac{2(\nu_m \nu_x)^{3/2}}{\nu} C_{mx}^\gamma$

(4)  $B_{mx}^\gamma = 2\beta^{(0)} + \frac{2\beta^{(1)}}{\alpha^2 I} \left[ 1 - \left( 1 + \alpha I^{1/2} - \frac{\alpha^2 I}{2} \right) \exp(-\alpha I^{1/2}) \right]$

(5)  $C_{mx}^\gamma = 3/2 C_{mx}^\phi$

Excess Gibbs Free Energy

(6)  $\Delta G^{ex} = n_w \nu m R T (1 - \phi + \ln \gamma_\pm)$

(7)  $\Delta G^{ex} = n_w R T \left[ -A_\phi \frac{4I}{1.2} \ln(1 + 1.2I^{1/2}) + m^2 \cdot 2\nu_m \nu_x B_{mx} + m^3 \cdot 2(\nu_m \nu_x)^{3/2} C_{mx} \right]$

(8)  $B_{mx} = \beta^{(0)} + \frac{2\beta^{(1)}}{\alpha^2 I} \left[ 1 - (1 + \alpha I^{1/2}) \exp(-\alpha I^{1/2}) \right]$

(9)  $C_{mx} = \frac{C_{mx}^\phi}{2}$

Relative Heat Capacity

(10)  $J = m\nu |Z_m Z_x| \frac{A_J}{3.6} \ln(1 + 1.2I^{1/2}) - 2\nu_m \nu_x R T^2 m^2 B_{mx}^J - 2(\nu_m \nu_x)^{3/2} R T^2 m^3 C_{mx}^J$

(11)  $J = C_{p1} - n_w \bar{C}_{p1}^0 - m \bar{C}_{p2}^0$

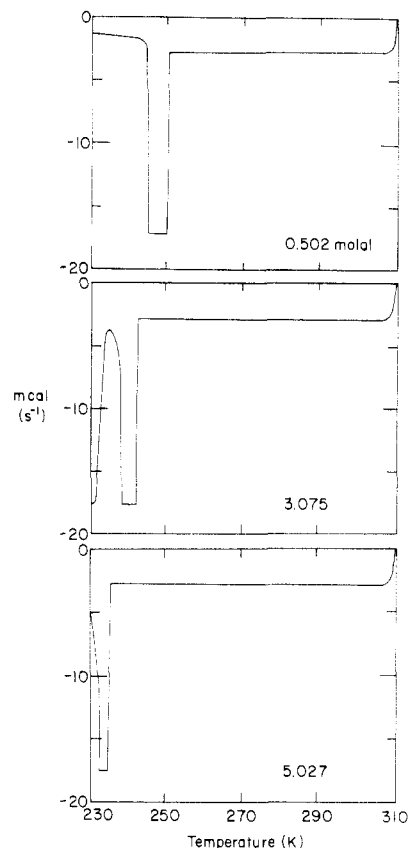
(12)  $B_{mx}^J = \left( \frac{\partial^2 B_{mx}}{\partial T^2} \right)_{P,I} + \frac{2}{T} \left( \frac{\partial B_{mx}}{\partial T} \right)_{P,I}$

$$= \left( \frac{\partial^2 \beta^{(0)}}{\partial T^2} \right)_P + \frac{2}{T} \left( \frac{\partial \beta^{(0)}}{\partial T} \right)_P + \left[ \left( \frac{\partial^2 \beta^{(1)}}{\partial T^2} \right)_P + \frac{2}{T} \left( \frac{\partial \beta^{(1)}}{\partial T} \right)_P \right] \left( \frac{2}{\alpha^2 I} \right) \left[ 1 - (1 + \alpha I^{1/2}) \exp(-\alpha I^{1/2}) \right]$$

(13)  $C_{mx}^J = \left( \frac{\partial^2 C_{mx}}{\partial T^2} \right)_P + \frac{2}{T} \left( \frac{\partial C_{mx}}{\partial T} \right)_P$

(14)  $A_J = \left( \frac{\partial A_H}{\partial T} \right)_P$

<sup>a</sup>Symbols:  $A_\phi$  = Debye-Hückel slope for the activity and osmotic coefficient.  $A_J$  = Debye-Hückel slope for heat capacity.  $Z_m Z_x$  = the charge on cation, anion respectively.  $\nu_m \nu_x$  = the number of cations and anions respectively per formula weight in a strong electrolyte mx.  $\alpha = 2.0$ , a constant.  $I$  = ionic strength,  $I = \frac{1}{2} m \cdot (\nu_m Z_m^2 + \nu_x Z_x^2)$ .  $n_w$  = kilograms of water.  $m$  = molality, moles of salt kg H<sub>2</sub>O<sup>-1</sup>.  $C_{p1}$  = total heat capacity, cal K<sup>-1</sup>.  $\bar{C}_{p1}^0$  = molal heat capacity of pure water, cal K<sup>-1</sup> mol<sup>-1</sup>.  $\bar{C}_{p2}^0$  = partial molal heat capacity of solute at infinite dilution, cal K<sup>-1</sup> mol<sup>-1</sup>.

**Figure 1.** Thermograms of cooling scans at different salt concentrations. The onset of freezing occurs at lower temperatures as the concentration increases.**Table III. Coefficients of Eq 3-5**

$x_1 = 7.66249$	$x_9 = 4.49459 \times 10^{-5}$
$x_2 = -1.00472 \times 10^3$	$x_{10} = -7.86640 \times 10^{-8}$
$x_3 = -1.79001 \times 10^{-3}$	$x_{11} = -5.34139 \times 10^{-1}$
$x_4 = 1.15601 \times 10^{-5}$	$x_{12} = 7.13101 \times 10^1$
$x_5 = -1.90346 \times 10^{-8}$	$x_{13} = 1.22262 \times 10^{-4}$
$x_6 = 2.57468 \times 10^1$	$x_{14} = -7.80262 \times 10^{-7}$
$x_7 = -3.25771 \times 10^3$	$x_{15} = 1.27174 \times 10^{-9}$
$x_8 = -6.58529 \times 10^{-3}$	

of  $\beta^{(0)}$ ,  $\beta^{(1)}$ , and  $C^\phi$  obtained reproduce the specific heat data to within 0.004 cal g<sup>-1</sup> K<sup>-1</sup>.

The temperature variation of the fitted parameters  $\partial^2 \beta^{(0)}/\partial T^2$ ,  $\partial^2 \beta^{(1)}/\partial T^2$ , and  $\partial^2 C^\phi/\partial T^2$  is most simply represented by second degree polynomials from 25 to -40 °C. The polynomial equations are integrated twice by using the values of  $\beta^{(0)}$ ,  $\beta^{(1)}$ , and  $C^\phi$  and their first temperature derivatives at 25 °C as the integration constants. Values of  $\beta^{(0)}$ ,  $\beta^{(1)}$ , and  $C^\phi$  at 25 °C are from White (8) and the first derivatives are from Silvester and Pitzer (5). The temperature dependence of the parameters is given by the following equations

$$\beta^{(0)} = 2x_1 + 2x_2/T + x_3 T^2/6 + x_4 T^3/12 + x_5 T^4/20 \quad (3)$$

$$\beta^{(1)} = 2x_6 + 2x_7/T + x_8 T^2/6 + x_9 T^3/12 + x_{10} T^4/20 \quad (4)$$

$$C_{mx} = 2x_{11} + 2x_{12}T + x_{13}T^2/6 + x_{14}T^3/12 + x_{15}T^4/20 \quad (5)$$

$$= C^\phi/2$$

The coefficients of eq 3-5 are listed in Table III.

Table IV. Values of  $\gamma^\pm$  and  $a_w$  Calculated below 0 °C in This Study

m	0 °C		-5 °C		-10 °C		-15 °C		-20 °C		-25 °C		-30 °C		-35 °C		-40 °C	
	$\gamma^\pm$	$a_w$	$\gamma^\pm$	$a_w$	$\gamma^\pm$	$a_w$	$\gamma^\pm$	$a_w$	$\gamma^\pm$	$a_w$	$\gamma^\pm$	$a_w$	$\gamma^\pm$	$a_w$	$\gamma^\pm$	$a_w$	$\gamma^\pm$	$a_w$
0.5	0.656	0.9839	0.646	0.9840	0.633	0.9842	0.618	0.9844	0.600	0.9846	0.580 <sup>a</sup>	0.9849 <sup>a</sup>	0.557 <sup>a</sup>	0.9852 <sup>a</sup>	0.513 <sup>a</sup>	0.9856 <sup>a</sup>	0.503 <sup>a</sup>	0.9860 <sup>a</sup>
1.0	0.614	0.9679	0.598	0.9684	0.578	0.9688	0.556	0.9694	0.530	0.9702	0.501 <sup>a</sup>	0.9710 <sup>a</sup>	0.469 <sup>a</sup>	0.9720 <sup>a</sup>	0.434 <sup>a</sup>	0.9731 <sup>a</sup>	0.397 <sup>a</sup>	0.9744 <sup>a</sup>
2.0	0.599	0.9347	0.574	0.9358	0.546	0.9372	0.513	0.9389	0.477	0.9408	0.438	0.9431	0.396 <sup>a</sup>	0.9458 <sup>a</sup>	0.352 <sup>a</sup>	0.9489 <sup>a</sup>	0.307 <sup>a</sup>	0.9526 <sup>a</sup>
3.0	0.623	0.8982	0.592	0.9001	0.556	0.9023	0.516	0.9049	0.473	0.9080	0.426	0.9117	0.377	0.9160	0.327 <sup>a</sup>	0.9210 <sup>a</sup>	0.278 <sup>a</sup>	0.9268 <sup>a</sup>
4.0	0.676	0.8576	0.639	0.8598	0.598	0.8624	0.552	0.8656	0.501	0.8693	0.448	0.8736	0.393	0.8788	0.337	0.8848	0.282 <sup>a</sup>	0.8918 <sup>a</sup>
5.0	0.756	0.8122	0.716	0.8142	0.670	0.8165	0.619	0.8193	0.563	0.8227	0.504	0.8266	0.443	0.8313	0.380	0.8368	0.319	0.8432
6.0	0.870	0.7620	0.829	0.7629	0.780	0.7641	0.726	0.7655	0.667	0.7673	0.603	0.7693	0.536	0.7718	0.467	0.7748	0.397	0.7784

<sup>a</sup> Indicates values exceed temperature range of heat capacity equations.

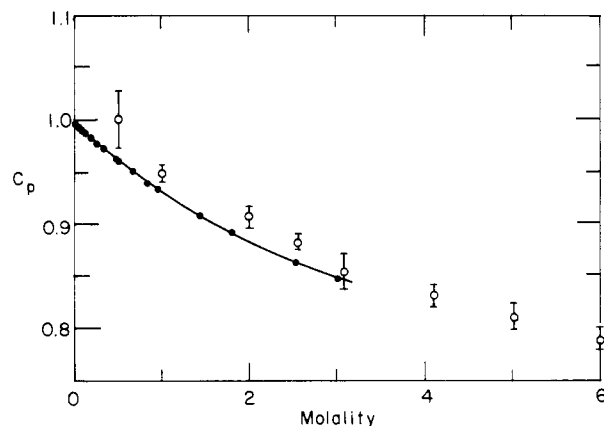


Figure 2. Comparison of specific heat values at 15 °C (O) with literature data (●) ( $\beta$ ) as a function of concentration.

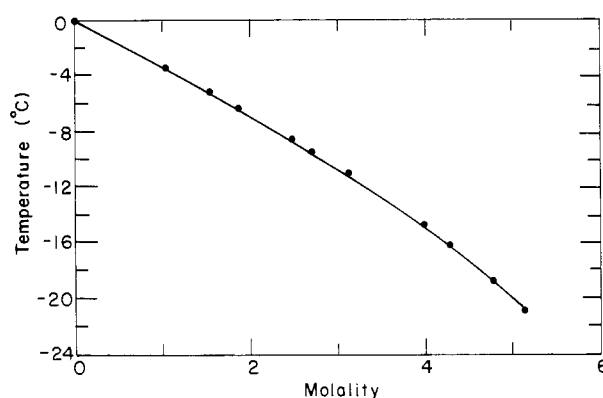


Figure 3. Comparison of the experimental freezing point of NaCl solutions (11) (solid line) with the values calculated from Pitzer's equations and low-temperature heat capacity data determined in this study (●).

Table V. Coefficients of Eq 11

$z_1 = 3.0256 \times 10^1$	$z_4 = 1.68746 \times 10^2$
$z_2 = -1.1274 \times 10^{-1}$	$z_5 = -3.49782 \times 10^3$
$z_3 = 1.2876 \times 10^{-4}$	

## Discussion

**Activities of NaCl and Water.** The mean activity coefficient of sodium chloride and activity of water were calculated from the ion interaction model (eq 1 and 3, Table II) with the values of  $\beta^{(0)}$ ,  $\beta^{(1)}$ , and  $C^\phi$  determined in this study (eq 3–5). Values of  $\gamma^\pm$  and  $a_w$  calculated over the entire temperature and concentration range of this study are listed in Table IV.

**Predicted Freezing Point below 0 °C.** The accuracy of the constants determined above can be checked by independently calculating  $a_w$  from the thermodynamic properties of ice. In a solution of sodium chloride at the freezing point

$$\Delta G_s^0(\text{ice}) = -RT \ln a_w \quad (6)$$

where  $\Delta G_s^0$  is the free energy change in going from ice to infinite dilution at some temperature,  $T$ .

To calculate the temperature dependence of  $\Delta G_s^0$ , the derivative with respect to temperature yields

$$\frac{\partial}{\partial T} \left( \frac{\Delta G_s^0}{T} \right) = \frac{-\Delta H_s^0}{T^2} \quad (7)$$

**Table VI. Activity of Water ( $a_w$ ) at Ice Saturation Compared to Values from  $\Delta G_s^0(\text{ice})$  and Experimental Solubilities**

$T, ^\circ\text{C}$	$a_w$		$\Delta$
	calcd	$\Delta G_s^0$	
-3.48	0.9666	0.9668	0.0002
-5.17	0.9515	0.9510	-0.0005
-6.32	0.9414	0.9405	-0.0009
-8.52	0.9222	0.9205	-0.0017
-9.41	0.9150	0.9126	-0.0024
-11.04	0.9007	0.8982	-0.0025
-14.77	0.8682	0.8660	-0.0022
-16.21	0.8562	0.8539	-0.0023
-18.73	0.8346	0.8331	-0.0015
-20.85	0.8129	0.8160	0.0031

where  $\Delta H_s^0$  is the heat of solution at infinite dilution. At 0 °C,  $\Delta H_s^0 = -1436$  cal. The variation of  $\Delta H_s^0$  is found from

$$\frac{\partial \Delta H_s^0}{\partial T} = \Delta C_p^0 \quad (8)$$

where  $\Delta C_p^0$  is the difference in heat capacity between ice and pure water.

$$\Delta C_p^0(\text{ice}) = C_{p,1}^0 - C_{p,(s)} \quad (9)$$

The values of  $C_{p,1}^0$  and  $C_{p,(s)}$  are from the measured heat capacities of water emulsions down to -38 °C (9) and the heat capacity of ice (10).

$$\Delta C_p^0(\text{ice}) = z_1 + z_2 T + z_3 T^2 \quad (10)$$

Integration of eq 10 with the values of  $\Delta H_s^0$  and  $\Delta G_s^0$  for ice at 0 °C gives

$$\Delta G_s^0(\text{ice}) = -z_1 T \ln T - \frac{z_2}{2} T^2 - \frac{z_3 T^3}{6} + z_4 T + z_5 \quad (11)$$

The coefficients of eq 11 are listed in Table V. A comparison of the activity of water calculated from the properties of ice and from Pitzer's equations by using the parameters determined above is given in Table VI. The average standard deviation is 0.0017. In Figure 3 the calculated solubility of ice is plotted against the experimental solubility (11) and reasonable agreement is obtained. These results show that Pitzer's equations can be used to assist estimates of thermodynamic properties of salts at freezing temperatures.

Registry No. NaCl, 7647-14-5; H<sub>2</sub>O, 7732-18-5.

#### Literature Cited

- (1) Pitzer, K. S. *J. Phys. Chem.* **1973**, *77*, 268-277.
- (2) Pitzer, K. S.; Kim, J. J. *Am. Chem. Soc.* **1974**, *96*, 5701-5707.
- (3) Rogers, P. S. Z.; Pitzer, K. S. *J. Phys. Chem.* **1981**, *85*, 2886-2895.
- (4) Silvester, L. F.; Pitzer, K. S. *J. Solution Chem.* **1976**, *7*(5), 327-337.
- (5) Silvester, L. F.; Pitzer, K. S. *J. Phys. Chem.* **1977**, *81*, 1822-1828.
- (6) Perron, G.; Fortier, J.-L.; Desnoyers, J. E. *J. Chem. Thermodyn.* **1975**, *7*, 1177.
- (7) Davis, J. C. *Statistics and Data Analysis in Geology*; Wiley: New York, 1973; p 413.
- (8) White, D. R.; Bates, R. G. *Aust. J. Chem.* **1980**, *33*, 1903-1908.
- (9) Angell, C. A.; Shuppert, J.; Tucker, J. C. *J. Phys. Chem.* **1973**, *77*, 3092-3099.
- (10) Dorsey, N. E. *Properties of Ordinary Water Substance*; Reinhold: New York, 1940; p 477.
- (11) Linke, N. F. *Solubilities of Inorganic and Metal Organic Compounds*; American Chemical Society: Washington, DC, 1958; p 958.

Received for review March 2, 1987. Accepted April 5, 1988. This research was supported by the Arctic Research Program, Division of Polar Programs, National Science Foundation, under Contract DPP-8200840.